RSC Sustainability

ROYAL SOCIETY OF CHEMISTRY

PAPER

View Article Online
View Journal | View Issue

Cite this: *RSC Sustainability*, 2026, **4**, 1901

Harnessing ketones as hydrogen acceptors for atom-efficient upgrading of oxygenates to fuels over H/ZSM-5

Jacob H. Miller, [a] Caleb A. Coatney, [a] Udishnu Sanyal, [b] Karthikeyan K. Ramasamy,[b] Hieu A. Doan,[c] Rajeev S. Assary, [c] Anh T. To [a] and Cody J. Wrasman *[a]

Heterogeneous mixtures of bio-derived oxygenates are promising feedstocks for synthetic aviation fuel (SAF), but conversion strategies for one common component—short-chain (C_{5-7}) internal ketones—are lacking. Previous work has shown that cyclization of ketones over H/ZSM-5 is limited by its high productivity of light paraffins. We study 4-heptanone upgrading over H/ZSM-5 and show that aromatics and olefins can be formed at high carbon yield when operating at up to 90% conversion. The yield of desirable products is not impacted by the introduction of a recycle stream of the unconverted 4-heptanone and other products with similar boiling points. We hypothesize, based on first-principles calculations, that the higher olefin yield is driven by the ease of hydrogen transfer to unreacted ketones as opposed to hydrogenating olefin products. We demonstrate how this ease of hydrogen transfer to ketones can be leveraged to enhance olefin selectivity in the conversion of methanol to olefins as well by co-feeding ketones. Olefinic products of the cyclization reaction are then oligomerized to a SAF blendstock to demonstrate an end-to-end ketone-to-SAF process facilitated by upgrading ketones over H/ZSM-5 at partial conversion with a recycle stream. The results of this work demonstrate a strategy to improve the carbon yield from bio-derived acids to SAF to over 75%, representing a relative improvement of more than 50% compared to previously reported data.

Received 26th October 2025
Accepted 17th February 2026

DOI: 10.1039/d5su00817d

rsc.li/rscsus

Sustainability spotlight

This work proposes a strategy to produce drop in aviation fuels from wet waste derived ketones. The details of this work specifically outline how changes in reactor operating conditions as well as the addition of a downstream oligomerization process can improve aviation fuel yields from ketones to over 75%. This advance supports goals 7, affordable and clean energy, and 12, responsible production and consumption, in the UN's sustainable development goals by producing aviation fuels that our previous work model to be cost competitive with fossil fuels from waste feedstocks.

Introduction

Production of transportation fuels from wet wastes has been identified as an economically attractive strategy to utilize low value materials like food waste, manure, and sewage sludge.[1] Several strategies have been developed to convert low-cost feedstocks into short-chain (C_{2-8}) carboxylic acids as intermediates for fuels production, including fermentation of biomass hydrolysate-derived sugars to butyric acid[2–4] and arrested anaerobic digestion of wet wastes to mixed carboxylic acids.[1,5,6] Carboxylic acids can be subsequently upgraded to ketones *via* ketonization over solid acid catalysts such as ZrO_2 and TiO_2.[7–13] Ketones in the aviation fuel range (C_{8-16}), can be readily hydrotreated to an *n*-paraffin SAF blendstock.[14,15] Shorter ketones (C_{3-7}) produced from ketonization of acetic, propanoic, and butyric acids need alternative processing steps to form aviation-range molecules. Several investigations have explored aldol condensation of these ketones over oxide catalysts.[16–20] However, these studies have largely been limited to methyl ketones, with Sun *et al.*[21] specifically noting that 3-pentanone, an internal (non-methyl) ketone, did not couple with itself over $MgZrO_x$. Other studies have suggested that steric hindrance limits the rate of condensation of internal ketones.[22]

An alternative pathway to aldol condensation is thus needed for upgrading streams rich in internal ketones with fewer than seven carbons. Fufachev *et al.*,[8] Cao *et al.*,[23] and Wang *et al.*[24] all recently explored an alternative pathway, reacting C_{5-7} ketones over H/ZSM-5 in an inert atmosphere to achieve up to 50%

[a]*Catalytic Carbon Transformation and Scale-Up Center, National Laboratory of the Rockies, Golden, CO 80401, USA. E-mail: cody.wrasman@nlr.gov*

[b]*Chemical and Biological Processing Group, Energy and Environment Directorate, Pacific Northwest National Laboratory, Richland, WA 99354, USA*

[c]*Material Science Division, Argonne National Laboratory, Lemont, IL 60439, USA*

carbon yields to aromatics. Alkyl aromatic molecules are valuable aviation fuel components that are necessary for achieving the elastomer seal swelling needed for engine operation.[25] This approach is also attractive because it produces a hydrocarbon product without the necessity of added H_2. Our group[26] recently observed a similar result during upgrading of a waste-derived mixture of carboxylic acids (primarily acetic and butyric) *via* ketonization and subsequent reaction over H/ZSM-5. We obtained a 49% carbon yield to valuable products (SAF-range aromatics; aromatic platform chemicals benzene, toluene, ethylbenzene, and xylenes (BTEX); and naphtha-range alkanes). Technoeconomic analysis indicated that the low carbon selectivity to SAF or BTEX was an economic barrier. In particular, the carbon yield of low value light ($<C_6$) alkanes exceeded 15% when the ketone feed was completely converted. High selectivity to alkanes is also known to be a challenge for the conversion of methanol to hydrocarbons over HZSM-5,[27,28] and is ascribed to hydrogen transfer from dehydrogenated species to olefins.[29]

In this work, we aim to understand what factors influence the formation of light alkane molecules and propose an improved process for converting C_{3-7} ketones into SAF. We report a strategy to obtain aromatic and branched hydrocarbon SAF blendstocks at high (>80%) yields from butyric acid, with the key step being reaction of 4-heptanone over H/ZSM-5 at incomplete conversion. We first analyzed the reaction network for 4-heptanone upgrading to show that at ketone conversions up to 90%, olefins are only sparingly hydrogenated to paraffins. We then confirmed that unreacted 4-heptanone can be recycled to the reactor influent along with C_{6-8} hydrocarbons of similar boiling point to form the same set of products as neat 4-heptanone feed. We next explored the low rate of light olefin hydrogenation to paraffins at incomplete reactant conversion, despite such hydrogenation occurring during methanol conversion over H/ZSM-5 at equivalent conditions.[30,31] To do this, we co-fed 4-heptanone and methanol over H/ZSM-5 and observed enhanced olefin selectivity compared to methanol alone. This confirmed that ketones can preserve olefins derived from other reactants, enhancing applicability of this SAF production pathway to non-carbonyl-containing reactants. We performed first-principles calculations of hydrogen affinity for relevant olefins and oxygenates to show that ketones are preferentially hydrogenated over olefins in zeolites. Finally, we demonstrated how recovered mixed olefins from the 4-heptanone cyclization can be oligomerized and hydrogenated into SAF range molecules.

Methods

Experimental

The H/ZSM-5 catalyst used in this work for both ketone upgrading and oligomerization was obtained from Zeolyst (CBV8014, Si/Al = 40) in NH_4 form and pretreated in stagnant air for 8 hours at 550 °C to convert to proton form. An X-ray diffractogram and N_2 physisorption isotherm of the catalyst are shown in Fig. S1. The Ni/SiO_2–Al_2O_3 oligomerization catalyst was prepared by incipient wet impregnation of $Ni(NO_3)_2$ on commercial SiO_2–Al_2O_3 (Davicat 3113 obtained from WR Grace). Ni content was 2 wt% as determined by inductive coupled plasma (ICP) analysis. Zeolites and Ni/SiO_2–Al_2O_3 were pelletized and sieved to particle sizes between 117–400 μm before use. Pt/C (10 wt% Pt) powder was obtained from Sigma-Aldrich and used for hydrogenation of oligomerized olefins. Reactant 4-heptanone was obtained from Sigma-Aldrich (98%) and filtered through a 0.45 μm PTFE filter disc before use. Reactant methanol was obtained from J.T. Baker (≥99.9%). Helium (Matheson Gas, 99.999%) was used as a sweep gas during vapor-phase reactions. Olefin reactants for oligomerization were obtained from Sigma-Aldrich (1-butene, 2-pentene, 1-pentene, 2-methyl-2-butene, and 1-hexene), Fisher Scientific (1-methylcyclopentene), and Oxarc (ethylene).

Reactions were performed in a Dursan-coated (SilcoTek Coating Co.) stainless steel packed-bed reactor heated by a clamshell furnace and described in our previous work.[7,26] Gases were fed with Brooks Instruments mass flow controllers and combined with liquids fed using a Chrom Tech high-pressure liquid chromatography (HPLC) pump in a 200 °C preheating zone upstream of the catalyst bed. Reaction mixtures were flowed downward through a catalyst bed containing 0.1–1 g catalyst supported by a glass wool plug. Temperature was monitored using a concentric thermocouple (Omega) placed inside the catalyst bed. A liquid-cooled heat exchanger operating at 2 °C condensed liquid products for collection in a knockout pot, which was emptied periodically (every 2–16 hours). Uncondensed gaseous products were monitored online using an Agilent 6890 gas chromatograph (GC) equipped with an HP-PLOT Q column and a thermal conductivity detector. Reactant feed rate was monitored by placing liquid feed reservoirs on Mettler Toledo mass balances and tracking mass changes over time, and liquid product mass was measured similarly. Liquid product samples contained both an organic and aqueous phase, which were separated and independently analyzed. Organic liquid products were diluted in acetone (usually 1 : 250 v/v), mixed with a nonane internal standard, and analyzed using an Agilent 7890A GC equipped with an Agilent HP-5 MS column, a 5975C mass spectrometer, and a Polyarc quantitative carbon detector (Activated Research Company/Shimadzu). Aqueous liquid products contained only water, except for in experiments with methanol feed. In those cases, aqueous products contained methanol and water; methanol content was determined *via* manual injection into the online Agilent 6890 GC. Catalyst coke was quantified using a Setaram Setsys Evolution thermogravimetric analysis (TGA) system. In these measurements, catalysts were heated to 110 °C at 5 °C min^{-1} and held for 30 minutes in an Al_2O_3 pan in flowing N_2 to remove adsorbed water. The gas composition was then changed to dry air (ZeroAir, Matheson) and the sample was heated to 800 °C at 10 °C min^{-1} while tracking changes in mass. The reactor system was equipped with a robust process monitoring system that tracks system pressure, temperature, and possible leakages, and shuts down if deviations from expected conditions occur, ensuring operator safety.

Mixed olefin oligomerization experiments were conducted using a fixed bed continuous flow reactor with a total of 2 g catalyst (dual bed catalyst containing 1 g of Ni/SiO_2–Al_2O_3 and H/ZSM-5). The feedstock consisted of an equimolar concentration of ethylene (C_2), propylene (C_3) and a premixed olefin blend

Table 1 Molar composition of mixed olefin liquid fed along with propylene and ethylene during the mixed olefin oligomerization

Olefin composition	Mole fraction
2-Pentene	0.326
2-Methyl-2-butene	0.239
Methylcyclopentene	0.157
1-Pentene	0.109
1-Hexene	0.169

of pentenes and hexenes (C_5/C_6). The detailed composition of C_5/C_6 olefin blend is shown in Table 1.

Carbon balances (CB) were measured using eqn (1) and were always closed within 80% and usually closed within 90%:

$$\mathrm{CB} = \frac{\sum_{i=\text{products, reactants}} C_{n,i}\dot{n}_i}{\sum_{i=\text{reactants}} C_{n,i}\dot{n}_{i,0}} \quad (1)$$

Here, $C_{n,i}$ is the carbon number of species i, $n_{i,0}$ is the influent molar flowrate of species i over a time interval, and n_i is the effluent molar flowrate of species i over the same time interval. Carbon yields of each product j (Y_j) were calculated using eqn (2):

$$Y_j = \frac{C_{n,j}\dot{n}_j}{\sum_{i=\text{reactants}} C_{n,i}\dot{n}_{i,0}} \quad (2)$$

Conversion of reactant i (X_i) when it was observed in the effluent during single-reactant experiments and overall carbon conversion in cofeed experiments was calculated using eqn (3):

$$X_i = \frac{\sum_{j=\text{products}} C_{n,j}\dot{n}_j}{\sum_{i=\text{reactants}} C_{n,i}\dot{n}_{i,0}} \quad (3)$$

Conversion was reported as full (100%) when no reactant was left in the effluent. Methanol is assumed to be in equilibrium with dimethyl ether (DME), its bimolecular dehydration product, during reactions of methanol, so DME was not counted as a product in conversion calculations. Conversion was defined for individual reactants in co-feed experiments using eqn (4):

$$X_i = \frac{\dot{n}_i}{\dot{n}_{i,0}} \quad (4)$$

Carbon selectivity of each product j (S_j) was calculated using eqn (5):

$$S_j = \frac{C_{n,j}\dot{n}_j}{\sum_{j=\text{products}} C_{n,j}\dot{n}_j} \quad (5)$$

We have shown previously *via* rigorous heat- and mass-transfer calculations that no significant mass or thermal gradients exist between the bulk gas phase and H/ZSM-5 catalyst particle surfaces (satisfying Mears' criteria).[32] Intraparticle mass transfer gradients do exist, but intraparticle thermal gradients do not.[26]

Computational methods

All gas-phase calculations were performed at the high-level G4MP2 level of theory[33,34] using the Gaussian 16 package.[35] The Gibbs free energies of protonation (ΔG_{prot}) were calculated using eqn (6):

$$\Delta G_{\mathrm{prot}} = G_{\mathrm{carbocation}} - G_{\mathrm{neutral}} - G_{\mathrm{H^+}} \quad (6)$$

where $G_{\mathrm{carbocation}}$ and, G_{neutral} are the computed Gibbs free energy of the optimized carbocation and the neutral olefin/oxygenate molecule, respectively. A value of -26.34 kJ mol^{-1} was used for the Gibbs free energy of the proton ($G_{\mathrm{H^+}}$).[36]

Results

Understanding the correlation between 4-heptanone conversion and paraffin selectivity

Previous work has suggested that the production of C_{2-6} paraffins is dependent on the level of 4-heptanone conversion.[26] To confirm this observation, the product slate of 4-heptanone reaction over H/ZSM-5 was measured at conversions between 20% and 100%. Fig. 1a shows the gradual deactivation of H/ZSM-5 with 4-heptanone exposure over three independent reactions performed in a packed-bed reactor. We showed in our recent publication that (i) the H/ZSM-5 catalyst can be regenerated after deactivation by exposure to air at 550 °C and (ii) catalyst deactivation is non-selective, meaning that selectivity of all products at a given 4-heptanone conversion will always be the same, regardless of catalyst deactivation.[26] Thus, a reaction network of 4-heptanone upgrading can be postulated by examining trends in product selectivity as a function of $X_{4\text{-heptanone}}$ over single experiments as the catalyst deactivates with time on stream.

Trends in selectivity of major product groups as a function of 4-heptanone conversion are shown to be consistent over multiple independent experiments in Fig. 1b. Catalyst coke selectivity was analyzed using thermogravimetric analysis and was determined to be below 1%. The postulated reaction network for upgrading of 4-heptanone to hydrocarbons has been described previously.[26] Briefly, 4-heptanone initially reacts *via* two pathways, either (i) dehydration to heptadienes or C_7 cyclic alkenes or (ii) C–C scission to light olefins. Fig. 1b shows that these two product groups (with heptadienes or C_7 cyclic alkenes accounting for most of the C_{7-8}, non-BTEX group) account for ~80% carbon selectivity at low $X_{4\text{-heptanone}}$ (25%, Fig. 1). Selectivity to both product groups declines with increasing conversion, showing that these products are subsequently converted into other molecules. The decrease in C_{7-8}, non BTEX selectivity is matched by a concomitant increase in selectivities for BTEX and C_{9+} aromatics, showing that the initially-formed C_7 products are aromatized and (in some cases) alkylated. Decreases in C_{2-6} olefin selectivity are matched by increases in C_{2-6} paraffin selectivity, showing that the primary consumption pathway for olefins is hydrogenation to paraffins.

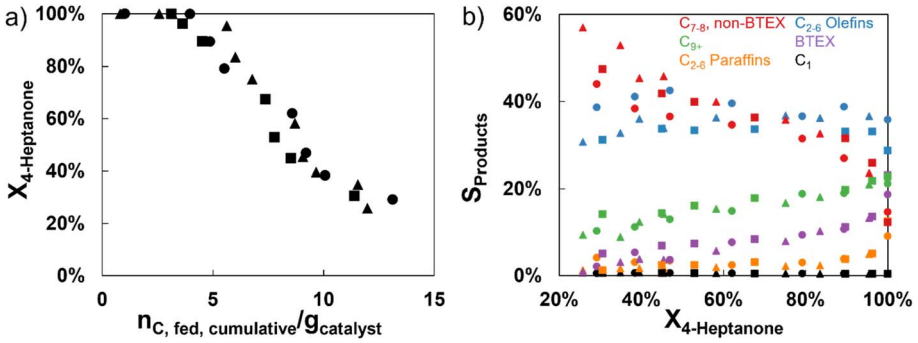

Fig. 1 Reaction results for 4-heptanone conversion over H/ZSM-5 during three independent flow reactions represented by circles, triangles, and squares. (a) Conversion of 4-heptanone ($X_{4\text{-heptanone}}$) as a function of cumulative carbon moles fed per H/ZSM-5 mass; (b) carbon selectivity of product categories as a function of $X_{4\text{-heptanone}}$. T: 350 °C, P_{total} = 200 kPa, $P_{4\text{-heptanone}}$ = 19 kPa, balance He (60–90 sccm), WHSV = 2.5–3 h^{-1}, $m_{H/ZSM\text{-}5}$ = 1 g.

Although C_{7-8} non-BTEX products and C_{2-6} olefins are both primary, unstable products, Fig. 1b shows that their selectivity trends with conversion are not equivalent. The selectivity of C_{7-8} non-aromatics decreases continuously with conversion, as would be expected for an unstable product consumed in a successive reaction. The selectivity of C_{2-6} olefins, meanwhile, stays relatively constant up to ~90% 4-heptanone conversion. This trend is illustrated clearly in Fig. 2 (black triangles, squares, and circles), which shows that the yield of C_{2-6} olefins as a share of all C_{1-6} products excluding benzene remains above 90% up to 90% 4-heptanone conversion (Fig. 2a), while the hydrogen transfer index (HTI), a measure of the fraction of C_{2-6} molecules that are saturated, remains below 10% up to the same conversion (Fig. 2b). Table S1 collects the mole fractions of all products with boiling points below 80 °C at 83% 4-heptanone conversion and shows that ethylene and propylene make up nearly 40 mol% of the light gases, followed by larger olefins. However, the fraction of C_{2-6} olefins in all C_{1-6} products decreased sharply above 90% 4-heptanone conversion, causing the HTI to increase to over 60%. This change indicates that conversions of 4-heptanone above 90% favor the rapid consumption of light olefins.

The difference in selectivity trends between C_{7-8}, non-BTEX molecules and C_{2-6} olefins is counterintuitive, as the former group's selectivity decreases steadily with increasing $X_{4\text{-heptanone}}$, while the latter group maintains relatively constant selectivity up to $X_{4\text{-heptanone}}$ ~ 85% and steeply declines at higher conversions (Fig. 2b). This contrast is particularly surprising because aromatization, the primary consumption mechanism of C_{7-8}, non-BTEX molecules, releases hydrogen. The transformation of C_{2-6} olefins into paraffins correspondingly requires hydrogen, but this transformation does not take place. Thus, an alternative hydrogen receptor must prevent light olefin hydrogenation until 4-heptanone conversion is close to complete.

Hydrogen affinity of ketones enhances olefin yields during zeolite upgrading

The "out of sync" trends in cycloalkane aromatization and olefin hydrogenation observed during 4-heptanone upgrading herein are not seen in all oxygenate upgrading reactions over H/ZSM-5. Methanol upgrading to hydrocarbons (MTH) over H/ZSM-5 is an extremely well-characterized reaction system, and many researchers including Bleken *et al.*[30] and Bjørgen *et al.*[31] have shown that olefin hydrogenation occurs quite readily

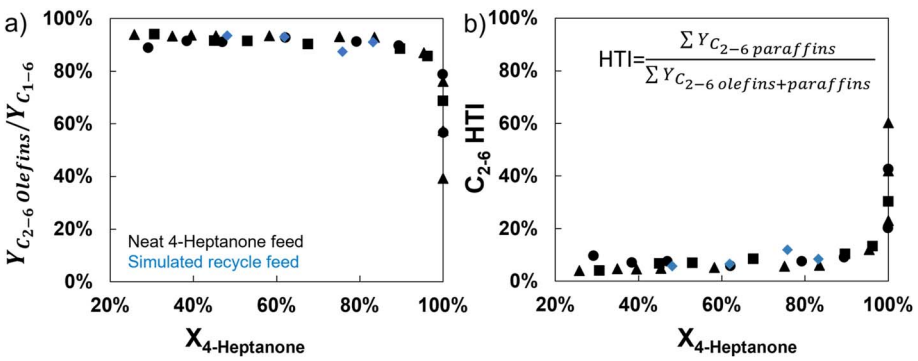

Fig. 2 Reaction results for 4-heptanone conversion over H/ZSM-5 during three independent flow reactions compared to a simulated recycle reaction. (a) Carbon ratio of olefins to all hydrocarbon products in the <80 °C boiling fraction; (b) C_{2-6} hydrogen transfer index (HTI). The three black shapes (triangles, squares, and circles) correspond to three independent reactions of 4-heptanone. T: 350 °C, P_{total} = 200 kPa, $P_{4\text{-heptanone}}$ = 19 kPa, balance He (60–90 sccm), WHSV = 2.5–3 h^{-1}, $m_{H/ZSM\text{-}5}$ = 1 g. Blue diamonds correspond to simulated recycle reaction. T: 350 °C, P_{total} = 160 kPa, He sweep gas (30 sccm), WHSV = 2–7 h^{-1}, $m_{H/ZSM\text{-}5}$ = 0.3 g. Y_{C1-6} includes all carbon-containing molecules with carbon numbers between 1–6 besides benzene.

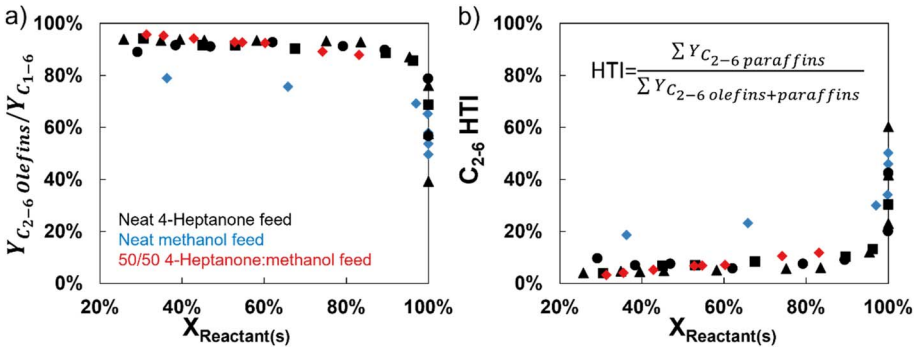

Fig. 3 Reaction results for 4-heptanone, methanol, and a blend of 4-heptanone and methanol conversion over H/ZSM-5 during five independent flow reactions. (a) Carbon ratio of olefins to all hydrocarbon products <80 °C boiling fraction; (b) C_{2-6} hydrogen transfer index (HTI). Three shapes (triangles, squares, and circles) correspond to three independent reactions of 4-heptanone, blue diamonds correspond to a reaction of methanol, and red diamonds correspond to a reaction of 50/50 (C : C) 4-heptanone : methanol. *T*: 350 °C, P_{total} = 170–200 kPa, He sweep gas flowrate = 60–90 sccm; WHSV = 2.5–3 h^{-1} (pure 4-heptanone), 30–31 h^{-1} (pure methanol), and 9–10 h^{-1} (4-heptanone/methanol mixture); $m_{H/ZSM-5}$ = 1 g (4-heptanone), 0.1 g (methanol), 0.2 g (4-heptanone/methanol mixture). Both methanol and dimethyl ether are counted as unconverted for the purposes of calculating conversion.

during MTH. We directly demonstrate that olefins are readily converted to paraffins during MTH in Fig. 3, which shows that, at sub-complete methanol conversions, the yield of olefins among C_{1-6} products is consistently 20% lower (Fig. 3a) and HTI of C_{2-6} products is more than three times higher (Fig. 3b) compared to the same conversions for 4-heptanone upgrading. However, olefin selectivity and HTI values converge for the two feedstocks near complete conversion. This indicates that olefins are more likely to be hydrogenated in the MTH reaction, while olefin hydrogenation is suppressed during 4-heptanone conversion. This finding remains true when a 50/50 (C : C) mixture of methanol and 4-heptanone is reacted over H/ZSM-5 as the olefin selectivity and HTI are nearly identical to that of a pure 4-heptanone reactant up to a carbon conversion of 80%, indicating that the presence of 4-heptanone suppresses olefin hydrogenation regardless of olefin source. Khare *et al.*[37] observed a similar drop in olefin hydrogenation when co-feeding acetaldehyde during MTH over H/ZSM-5. Carbon yields of all observed product categories are collected in Fig. S2–S4 while the overall carbon conversions for the three feedstocks as a function of time on stream are compared in Fig. S5. These results demonstrate that neat 4-heptanone and the 50/50 mixture of 4-heptanone and methanol deactivated at a similar rate and had similar aromatic productivities. The neat methanol feed on the other hand took longer to begin deactivation but deactivated at a faster rate once it started. Furthermore, the methanol alone feed lost nearly all single ring aromatic selectivity once it began to deactivate while 4-heptanone containing feeds maintained higher yields of aromatic products, suggesting that 4-heptanone encouraged the formation of aromatic products.

We hypothesize that the rerouting of hydrogen transfer pathways causes carbonyl-containing compounds to promote olefin selectivity at the expense of paraffin formation during reactions over H/ZSM-5. It is well established that reactions of (i) cyclic hydrocarbons to aromatics and (ii) alcohols to aldehydes or ketones (*e.g.*, methanol to formaldehyde) are the two pathways responsible for dihydrogen production during hydrocarbon and oxygenate reactions over H/ZSM-5 and other acid catalysts.[17,38–41] We do not observe H_2 in our reactor effluent, however, and it is not usually observed during reactions over acidic catalysts with no metal functionality under the reactor conditions studied here. Thus, hydrogenation and dehydrogenation reactions must be coupled (hydrogen transfer); every dehydrogenation reactant must transfer two H-atoms to a hydrogen acceptor.

Molecules with non-aromatic double bonds make ideal hydrogen acceptors; thus, relevant acceptors involved in 4-heptanone upgrading are ketones (4-heptanone itself) and olefins. DeLuca *et al.*[42] recently showed in a computational study that barriers for hydrogenation reactions over zeolites are correlated with stability of carbocations formed *via* protonation of the hydrogen acceptors double bond. Specifically, a lower Gibbs free energy of protonation (ΔG_{prot}) indicates a more stable carbocation or higher hydrogen affinity. We employed this logic to gauge the ease of hydrogenation among olefins and oxygenates: using accurate G4MP2 method to evaluate ΔG_{prot} of 4-heptanone, methanol, and C_{2-5} alkenes observed during 4-heptanone upgrading and MTH (Fig. 4a). The ΔG_{prot} of 4-heptanone is 10 kJ mol^{-1} less than that of any alkene considered (−835 kJ mol^{-1} *versus* −825 kJ mol^{-1} or higher) and significantly less than the ΔG_{prot} of propylene (−757 kJ mol^{-1}) and ethylene (−674 kJ mol^{-1}), the two olefins with the highest selectivity (Table S1). This is in stark contrast with methanol, which has a much higher value of ΔG_{prot} (−747 kJ mol^{-1}). These results indicate that hydrogenation of 4-heptanone is more favorable compared to other olefins and oxygenates. Indeed, Ji *et al.*[43] and Khare *et al.*[37] both also concluded that aldehydes and ketones are preferentially hydrogenated during oxygenate upgrading over zeolites. Fig. 4b illustrates the implications of this finding: when 4-heptanone is present in significant quantities, it will be hydrogenated instead of olefins. This reaction forms 4-heptanol, which rapidly dehydrates to 3-heptene. This molecule will either aromatize or crack to light olefins and

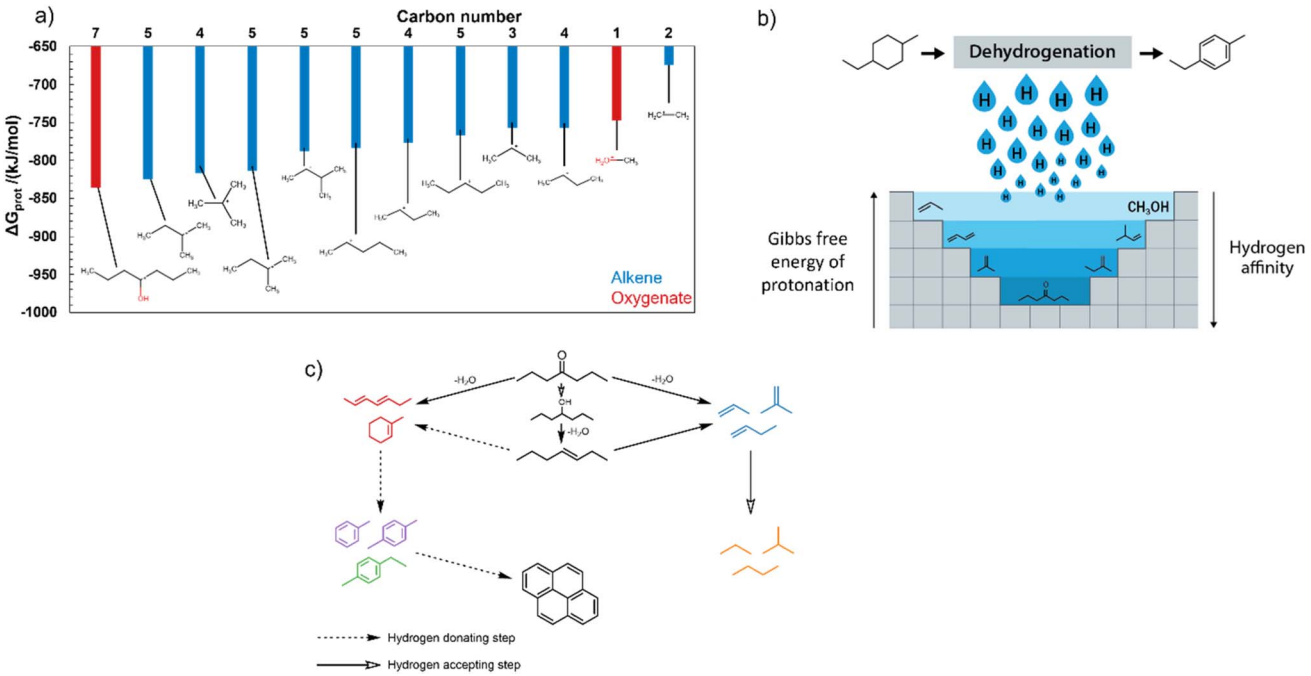

Fig. 4 (a) Comparison of calculated Gibbs free energy of protonation (ΔG_{prot}) of olefins and oxygenates observed during 4-heptanone upgrading and MTH. (b) Schematic of hydrogen transfer from aromatizing cycloalkanes to oxygenates and alkenes, where molecules capable of forming stable carbenium ions (low ΔG_{prot}) are advantaged hydrogen acceptors. (c) Simplified reaction network for 4-heptanone upgrading, highlighting steps involving hydrogen donation and acceptance. Molecule colors correspond to product lump colors in Fig. 1b.

paraffins, as shown in Fig. 4c. C_7 alcohol or olefin products of hydrogen transfer to 4-heptanone are difficult to observe directly because they are highly reactive and diffusionally constrained and thus unlikely to egress from the zeolite intact. We do not observe any 4-heptanol, likely due to its rapid dehydration. Fig. S6 compares the yields of other C_7 products during reactions of 4-heptanone, methanol, and the 50/50 (C : C) mixed feed shown in Fig. 4. C_7 yields are 3–4 times higher during reactions of 4-heptanone than the other reactants (Fig. S6a), primarily from formation of C_7H_{12} species (Fig. S6b), which can come from either dehydration of 4-heptanol or dehydrogenation of 4-heptanol-derived heptene, providing no way to distinguish between the two reaction pathways. Toluene (Fig. S6c) is also formed at higher yields when pure 4-heptanone is fed compared to methanol or mixtures. Yields of C_7H_{14} species, our hypothesized primary product of 4-heptanol dehydration, are low (<1%, Fig. S6d) during every reaction, although maximum yields (observed between 50–80% reactant conversion) increase slightly from 0.64 C% without 4-heptanone to 0.93 C% with 4-heptanone as the feed. These species could, however, be formed *via* alternative pathways such as C–C bond formation between olefins. The low-to-nonexistent yields of obvious 4-heptanone hydrogenation products (4-heptanol and C_7H_{14} species) indicates their high reactivity in the zeolite.

Fig. 4c also shows that cracking of C_7H_{14} species can form olefins. We show in Fig. S7 the yields of all C_{2-6} products (Fig. S7a), olefins (Fig. S7b), and paraffins (Fig. S7c) as a function of reactant conversion. Feeds of methanol result in higher yields of all these products compared to mixed 4-heptanone/methanol feeds or solely 4-heptanone, making assignment of olefins as products of cracking of a specific C_7 species difficult. Olefins can be formed from 4-heptanone cracking as well as C_7H_{14} cracking, although the former reaction necessitates production of equimolar amounts of dienes and olefins, as shown in eqn (7a) and (7b):

$$C_7H_{14}O \rightarrow H_2O + C_nH_{2n-2} + C_mH_{2m}\ (n + m = 7) \quad (7a)$$

$$C_7H_{14} \rightarrow C_nH_{2n} + C_mH_{2m}\ (n + m = 7) \quad (7b)$$

We do not observe significant production of any dienes with carbon numbers below C_7 during 4-heptanone reactions, showing that either (i) the major production route for olefins is through cracking of heptenes derived from 4-heptanone hydrogenation or (ii) dienes of chain lengths below C_7 are rapidly consumed *via* hydrogenation or aromatization. Since it is unlikely that C_7 dienes, which are observed, are uniquely resilient compared to dienes of lower carbon number, we posit that (i) is true and that observed olefin production results from cracking of 4-heptanone hydrogenation-derived heptenes *via* the following sequence of reactions:

$$C_7H_{14}O + RH_2 \rightarrow C_7H_{15}OH + R \quad (8a)$$

$$C_7H_{15}OH \rightarrow C_7H_{14} + H_2O \quad (8b)$$

$$C_7H_{14} \rightarrow C_nH_{2n} + C_mH_{2m}\ (n + m = 7) \quad (8c)$$

In eqn (8a), RH_2 is a hydrogen donor and R is its dehydrogenated analogue. Fig. S7b shows more evidence for the hypothesis of hydrogen transfer to 4-heptanone enhancing olefin selectivity, as olefin yields at low (<60%, and especially <30%) reactant conversion are higher when 4-heptanone and methanol are co-fed than when either is individually fed. This is likely because 4-heptanone is accepting hydrogen from methanol dehydration to formaldehyde at these conditions,[40,41] increasing flux of carbon through the pathway in eqn (8).

If no 4-heptanone is present (as in the case of a neat methanol feed), olefins will be hydrogenated to paraffins. This results in higher paraffin yields at equivalent conversions using pure methanol feeds than feeds containing 4-heptanone as shown in Fig. S7c and as a higher HTI in Fig. 3b. Olefins that form the lowest-energy carbocations upon protonation are preferentially hydrogenated. Fig. 4c illustrates the role of 4-heptanone in the reaction network as a H-acceptor and highlights steps which release hydrogen (C_7H_{12} aromatization, aromatic growth to deactivation-causing polyaromatics, and heptane dehydrogenation) and accept hydrogen (4-heptanone and olefin hydrogenation).

The trend in H-acceptor energy explains the data in Fig. 1–3. While 4-heptanone is abundant in the zeolite ($X_{4\text{-heptanone}}$ < 90%), selectivity to olefins is high (30–40%) while selectivity to paraffins (<5%) and HTI (<10%) are both low. This trend is not seen for methanol, a molecule with a much higher ΔG_{prot}. However, as 4-heptanone becomes scarce ($X_{4\text{-heptanone}}$ > 90%), paraffin selectivity and HTI both rapidly increase, such that the HTIs of both methanol and 4-heptanone upgrading converge at full reactant conversion (Fig. 3b).

The hydrogen uptake of 4-heptanone can also be empirically observed by examining products of 4-heptanone aromatization *via* reactions such as eqn (9):

$$C_7H_{14}O \rightarrow C_7H_8 + H_2O + 2[H_2] \quad (9)$$

In eqn (9), $[H_2]$ is placed in brackets because no H_2 is observed; hydrogen transfer to other molecules is facile. Following the analysis of Khare *et al.*,[37] if olefins were the only hydrogen acceptors available, we should expect to see two paraffins formed by olefin hydrogenation for every aromatic. However, the ratio of paraffins to aromatics is much lower than this, below 0.5 up to 99% $X_{4\text{-heptanone}}$, showing hydrogenation of a different molecule must be occurring. Our analysis herein shows that this hydrogen acceptor is 4-heptanone and that the presence of this ketone during oxygenate upgrading over H/ZSM-5 results in uniquely high C_{2-6} olefin selectivities, enabling upgrading of butyric acid and other similar molecules to aromatic SAF and olefins.

Oligomerization of simulated olefin stream offers increased aviation fuel yields

The above findings demonstrate that operation of the 4-heptanone conversion reactor at partial (below 80%) conversion leads to improved light olefin selectivity. However, these light olefins require further processing to become liquid transportation fuels. Several ASTM approved SAF concepts, including the alcohol to jet pathway, rely on oligomerization and hydrotreating to convert olefins into SAF-range alkanes.[44–47] Scheme 1 shows how the application of this concept can be incorporated into our previously-developed strategy to upgrade volatile fatty acids with fewer than four carbon atoms, such as butyric acid, into a SAF blendstock containing both aromatic and iso-alkane components. Briefly, butyric acid is ketonized over ZrO_2 to 4-heptanone in a packed-bed reactor, as has been demonstrated in previous work from our group and others.[7–9,15,26] The product 4-heptanone is, after separation from co-products CO_2 and water, fed to a reactor containing H/ZSM-5 operated at 80% conversion. Since H/ZSM-5 deactivates with time on stream under these conditions (Fig. 1a),[24,26,48] this reactor would need to allow for regular catalyst regeneration (validated in our previous work)[26] and could take forms such as a swing bed or moving bed. The partially converted effluent of the ketone upgrading reactor would be separable into four streams: water, light and naphthenic hydrocarbons (primarily olefins) with boiling points <80 °C, C_{9+} aromatics and polyaromatics with boiling points >144 °C, and a middle hydrocarbon stream consisting of unreacted 4-heptanone with BTEX and C_{7-8} non-aromatic molecules. The aqueous phase can be decanted, and the remaining three hydrocarbon streams could be separated *via* distillation.

The heavy C_{9+} aromatic stream can be used directly as a SAF blendstock, as shown in our previous work.[26] Fig. 2a shows that the light stream (boiling points < 80 °C) consists of ~90% alkenes, which can be oligomerized and hydrotreated to a mixture of jet- and diesel-range iso-alkanes (see below). This stream will also contain a small percentage of light alkanes, which can either be burned for process heat or, if desired, alkylated with the oligomer stream before hydrotreating to further increase carbon yield to fuels.[49,50] The unreacted 4-heptanone, BTEX, and C_{7-8} non-aromatic molecules can be recycled into the H/ZSM-5 reactor influent. BTEX molecules could also be separated from this stream using an additional extraction method, as suggested by Yadav *et al.*,[26,51] but we exclude this step from our proposed strategy. Scheme 1 shows the carbon selectivity to each effluent stream, assuming ideal separations and using H/ZSM-5 reactor effluents at 80% conversion described in Fig. 1. Under this scheme, 82.2% of influent carbon exits the system as SAF and diesel fuel, a marked improvement from the 49% carbon yield from C_{2-4} carboxylic acids to SAF, BTEX, and naphtha that we previously demonstrated using H/ZSM-5 at full conversion.[26]

The efficacy of the strategy shown in Scheme 1 hinges on the performance of two steps: (i) upgrading a recycled feed of 4-heptanone, BTEX, and C_{7-8} hydrocarbons over H/ZSM-5 with the same performance as neat 4-heptanone and (ii) complete oligomerization of the primarily olefinic stream of products with boiling point <80 °C from the H/ZSM-5 ketone upgrading reactor. We tested upgrading of a recycled feed by collecting and combining liquid partial conversion products of the three pure 4-heptanone reactions shown in Fig. 1 and 2 into the mixture shown in Table S2. The mixture contained mostly 4-heptanone (74.4 C%), with a balance of C_{7-8} non-BTEX hydrocarbons (18.3 C%) and <3 C% each of BTEX, C_{9+} aromatics, C_{2-6} olefins, and C_{2-6} paraffins. The 4-heptanone content of this mixture is

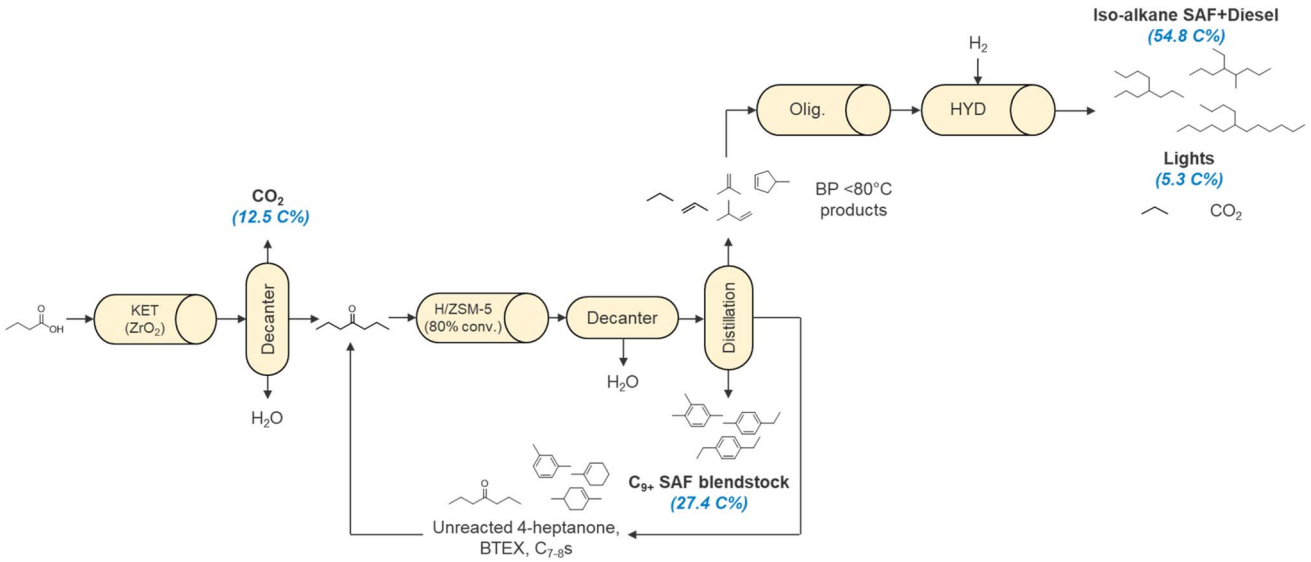

Scheme 1 Conceptual design of a process to upgrade butyric acid to SAF and diesel fuel based on experimental results. Bolded molecule categories show final products of the process; carbon selectivities to these are displayed in blue parentheses below each product. KET = ketonization, Olig. = oligomerization, and HYD = hydrogenation.

equivalent to running the H/ZSM-5 reactor at 80% 4-heptanone conversion and a recycle ratio (mass flow of recycle stream/mass flow of reactor inlet stream) of 0.84. Catalytic performance of this mixture (blue diamonds) is compared to that of neat 4-heptanone (black triangles, squares, and circles) in Fig. 2, where the trends in yield of C_{2-6} olefins as a share of C_{1-6} products (Fig. 2a) and C_{2-6} HTI (Fig. 2b) are shown to be identical between the simulated recycle and neat 4-heptanone reactor feeds. Production of C_{9+} aromatics also remains unchanged at these simulated recycle conditions. Thus, H/ZSM-5 is effective at upgrading a mixed feed of 4-heptanone and hydrocarbon products with boiling points between 80 and 144 °C to the same products as neat 4-heptanone.

The second critical step for the process is oligomerization of the olefin effluent of the H/ZSM-5 reactor. The content of the boiling point <80 °C stream at $X_{4\text{-heptanone}} = 83\%$, the proposed inlet to an oligomerization process, is shown in Table S1 and shows that $<C_6$ olefins make up over 84 mol% of the stream. We next oligomerized a representative mixture of olefins using a stacked bed reactor composed of (i) Ni/SiO_2–Al_2O_3 and (ii) H/ZSM-5. This proof-of-concept experiment was carried out using a feedstock of ethylene, 1-butene, 1-pentene, 2-pentene, 2-methyl-2-butene, methylcyclopentene and 1-hexene. Ethylene oligomerization proceeded *via* a Cossee–Arlman pathway over the Ni catalyst, while the C_{4+} alkenes from both the original feed and ethylene oligomerization were oligomerized over the downstream zeolite *via* acid-catalyzed pathways.[52,53] Performance and catalyst stability during oligomerization were monitored by the change in ethylene conversion over time as it can be measured unambiguously. Fig. 5a shows ~95% of ethylene conversion was obtained at the beginning of the reaction; however, conversion decreased continuously over time. Detailed analysis of the liquid product showed that selectivity to jet range compounds *i.e.*, C_8–C_{16} hydrocarbons was 65% and 53% after 25 and 45 h respectively (blue bars in Fig. 5a). Next, the oligomerized olefins (samples collected after

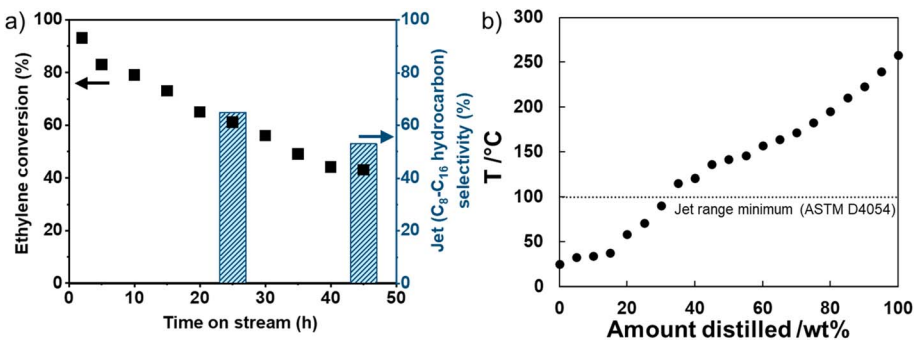

Fig. 5 (a) Ethylene conversion (black square) and jet (C_8–C_{16} olefins) selectivity (blue bar) obtained during mixed olefin oligomerization (T = 250 °C; P = 21 bar; WHSV = 0.7 h^{-1}) and (b) simulated distillation (ASTM D2887) of isoparaffin products of olefin oligomerization and hydrotreating (samples corresponding to 25 h demonstrated in Fig. 3a was used herein for analysis).

25 h) were hydrotreated in a lab-scale trickle-bed reactor over 10 wt% Pt/C (T = 250 °C, P_{H_2} = 3500 kPa, WHSV = 0.9 h^{-1}). Roughly half of the fed oligomers were transformed into SAF-range isoparaffins, as 67% of the mass fed to the reactor was recovered, while Fig. 5b shows that 65% of collected products were in the jet range (100–330 °C as defined for Simulated Distillation by ASTM D4054 (ref. 54)). All non-SAF products were light paraffins derived from non- or under-oligomerized olefins. The results herein highlight the feasibility of oligomerization to upgrade the light olefin mixture to SAF. Focused research is currently underway to optimize performance and identify the cause of oligomerization catalyst deactivation.

Conclusions

This work showed that carbonyl-containing organic reactants such as 4-heptanone can be reacted over H/ZSM-5 at incomplete conversion to form aromatic and (*via* subsequent light olefin oligomerization) isoparaffinic SAF blendstocks at high carbon yield. Our studies of the 4-heptanone upgrading reaction network evinced high olefin and aromatic selectivity up to 90% reactant conversion. Co-feeds of 4-heptanone with upgrading products with similar boiling points showed no difference in product distribution, meaning that these products can be recycled to the H/ZSM-5 reactor influent. First-principles calculations showed that the high hydrogen affinity of ketones attenuates olefin hydrogenation until most ketones are converted while co-feed experiments with 4-heptanone and methanol proved that even olefins derived from non-ketone sources can be preserved from hydrogenation by ketones. Finally, this work also demonstrated the feasibility of oligomerizing light olefins into alkane SAF-range molecules using a single mixed catalyst bed. Overall, these experiments outline a potential strategy to convert over 80% of the carbon in $<C_7$ ketones into liquid fuels. This result enhances the overall fuel yields in the carboxylic acids upgrading pathway by converting internal ketones into fuels.

Conflicts of interest

The authors declare that they have no known competing financial interests or personal relationships that could have appeared to influence this work.

Data availability

All data supporting the findings of this study are included within the paper and the supplementary information (SI), and the raw data will be made available by the authors upon request. Supplementary information is available. See DOI: https://doi.org/10.1039/d5su00817d.

Acknowledgements

This research was conducted as part of the ChemCatBio Consortium Catalytic Upgrading of Biochemical Intermediates project sponsored by the US Department of Energy – Office of Energy Efficiency and Renewable Energy, Bioenergy Technologies Office (BETO). Work at the National Laboratory of the Rockies was performed under Contract DE347AC36-99GO10337. Work at Argonne National Laboratory was performed under Contract DE-AC02-06CH11357. Work at Pacific Northwest National Laboratory was performed under Contract was performed at the Pacific Northwest National Laboratory (PNNL) under Contract no. DE-AC05-76RL01830. HAD and RSA acknowledge Consortium for Computational Physics and Chemistry (CCPC) for funding. HAD and RSA acknowledge the computing resources provided by the Laboratory Computing Resource Center at Argonne National Laboratory. The views expressed in the article do not necessarily represent the views of the U.S. Department of Energy or the U.S. Government. The U.S. Government retains and the publisher, by accepting the article for publication, acknowledges that the U.S. Government retains a nonexclusive, paid-up, irrevocable, worldwide license to publish or reproduce the published form of this work, or allow others to do so, for U.S. Government purposes. Neither the U.S. Government nor any agency thereof, nor any of their employees, makes any warranty, expressed, or implied, or assumes any legal liability or responsibility for the accuracy, completeness, or usefulness of any information, apparatus, product, or process disclosed, or represents that its use would not infringe privately owned rights.

References

1 M. R. Wiatrowski, *et al.*, Economic and sustainability prospects for wet waste valorization: The case for sustainable aviation fuel from arrested anaerobic digestion, *Renewable Energy*, 2024, **232**, 121063.
2 D. Salvachúa, *et al.*, Process intensification for the biological production of the fuel precursor butyric acid from biomass, *Cell Rep. Phys. Sci.*, 2021, **2**, 100587.
3 P. O. Saboe, *et al.*, Energy and techno-economic analysis of bio-based carboxylic acid recovery by adsorption, *Green Chem.*, 2021, **23**, 4386–4402.
4 P. O. Saboe, *et al.*, In situ recovery of bio-based carboxylic acids, *Green Chem.*, 2018, **20**, 1791–1804.
5 X. Ge, Y. Chen, V. Sànchez i Nogué and Y. Li, Volatile Fatty Acid Recovery from Arrested Anaerobic Digestion for the Production of Sustainable Aviation Fuel: A Review, *Fermentation*, 2023, **9**, 821.
6 A. H. Bhatt, Z. Ren and L. Tao, Value Proposition of Untapped Wet Wastes: Carboxylic Acid Production through Anaerobic Digestion, *iScience*, 2020, **23**, 101221.
7 J. H. Miller, G. R. Hafenstine, H. H. Nguyen and D. R. Vardon, Kinetics and Reactor Design Principles of Volatile Fatty Acid Ketonization for Sustainable Aviation Fuel Production, *Ind. Eng. Chem. Res.*, 2022, **61**, 2997–3010.
8 E. V. Fufachev, B. M. Weckhuysen and P. C. A. Bruijnincx, Toward Catalytic Ketonization of Volatile Fatty Acids Extracted from Fermented Wastewater by Adsorption, *ACS Sustain. Chem. Eng.*, 2020, **8**, 11292–11298.
9 B. Boekaerts and B. F. Sels, Catalytic advancements in carboxylic acid ketonization and its perspectives on

biomass valorisation, *Appl. Catal., B*, 2020, 119607, DOI: 10.1016/j.apcatb.2020.119607.
10 Q. Cai, *et al.*, Aqueous-Phase Acetic Acid Ketonization over Monoclinic Zirconia, *ACS Catal.*, 2018, **8**, 488–502.
11 M. Delarmelina, G. Deshmukh, A. Goguet, C. R. A. Catlow and H. Manyar, Role of Sulfation of Zirconia Catalysts in Vapor Phase Ketonization of Acetic Acid, *J. Phys. Chem. C*, 2021, **125**, 27578–27595.
12 E. V. Fufachev, B. M. Weckhuysen and P. C. A. Bruijnincx, Crystal Phase Effects on the Gas-Phase Ketonization of Small Carboxylic Acids over TiO_2 Catalysts, *ChemSusChem*, 2021, **14**, 2710–2720.
13 S. Wang and E. Iglesia, Experimental and theoretical assessment of the mechanism and site requirements for ketonization of carboxylic acids on oxides, *J. Catal.*, 2017, **345**, 183–206.
14 W. W. McNeary, *et al.*, Atomic Layer Deposition with TiO_2 for Enhanced Reactivity and Stability of Aromatic Hydrogenation Catalysts, *ACS Catal.*, 2021, **11**, 8538–8549.
15 N. A. Huq, *et al.*, Toward net-zero sustainable aviation fuel with wet waste-derived volatile fatty acids, *Proc. Natl. Acad. Sci. U. S. A.*, 2021, **118**, e2023008118.
16 S. Luo and J. L. Falconer, Acetone and acetaldehyde oligomerization on TiO_2 surfaces, *J. Catal.*, 1999, **185**, 393–407.
17 B. Oliver-Tomas, M. Renz and A. Corma, Direct conversion of carboxylic acids (C_n) to alkenes (C_{2n-1}) over titanium oxide in absence of noble metals, *J. Mol. Catal. A: Chem.*, 2016, **415**, 1–8.
18 M. Balakrishnan, *et al.*, Novel pathways for fuels and lubricants from biomass optimized using life-cycle greenhouse gas assessment, *Proc. Natl. Acad. Sci. U. S. A.*, 2015, **112**, 7645–7649.
19 E. R. Sacia, *et al.*, Highly Selective Condensation of Biomass-Derived Methyl Ketones as a Source of Aviation Fuel, *ChemSusChem*, 2015, **8**, 1726–1736.
20 B. Rozmysłowicz, *et al.*, Catalytic valorization of the acetate fraction of biomass to aromatics and its integration into the carboxylate platform, *Green Chem.*, 2019, **21**, 2801–2809.
21 J. Sun, S. Shao, X. Hu, X. Li and H. Zhang, Synthesis of Oxygen-Containing Precursors of Aviation Fuel via Carbonylation of the Aqueous Bio-oil Fraction Followed by C–C Coupling, *ACS Sustainable Chem. Eng.*, 2022, **10**, 11030–11040.
22 M. Balakrishnan, *et al.*, Novel pathways for fuels and lubricants from biomass optimized using life-cycle greenhouse gas assessment, *Proc. Natl. Acad. Sci. U. S. A.*, 2015, **112**, 7645–7649.
23 J. Cao, *et al.*, Conversion of C_{2-4} Carboxylic Acids to Hydrocarbons on HZSM-5: Effect of Carbon Chain Length, *Ind. Eng. Chem. Res.*, 2019, **58**, 10307–10316.
24 X. Wang, *et al.*, Conversion of propionic acid and 3-pentanone to hydrocarbons on ZSM-5 catalysts : Reaction pathway and active site, *Appl. Catal., A*, 2017, **545**, 79–89.
25 A. Anuar, V. K. Undavalli, B. Khandelwal and S. Blakey, Effect of fuels, aromatics and preparation methods on seal swell, *Aeronaut. J.*, 2021, **125**, 1542–1565.
26 J. H. Miller, *et al.*, Catalytic upgrading of wet waste-derived carboxylic acids to sustainable aviation fuel and chemical feedstocks, *EES Catal.*, 2024, **2**, 1111–1125.
27 F. L. Bleken, T. V. W. Janssens, S. Svelle and U. Olsbye, Product yield in methanol conversion over ZSM-5 is predominantly independent of coke content, *Microporous Mesoporous Mater.*, 2012, **164**, 190–198.
28 M. Bjørgen, *et al.*, Methanol to gasoline over zeolite H-ZSM-5: Improved catalyst performance by treatment with NaOH, *Appl. Catal., A*, 2008, **345**, 43–50.
29 S. Ilias and A. Bhan, Mechanism of the Catalytic Conversion of Methanol to Hydrocarbons, *ACS Catal.*, 2013, **3**, 18–31.
30 F. L. Bleken, T. V. W. Janssens, S. Svelle and U. Olsbye, Product yield in methanol conversion over ZSM-5 is predominantly independent of coke content, *Microporous Mesoporous Mater.*, 2012, **164**, 190–198.
31 M. Bjørgen, *et al.*, Methanol to gasoline over zeolite H-ZSM-5: Improved catalyst performance by treatment with NaOH, *Appl. Catal., A*, 2008, **345**, 43–50.
32 D. E. Mears, Diagnostic criteria for heat transport limitations in fixed bed reactors, *J. Catal.*, 1971, **20**, 127–131.
33 L. A. Curtiss, P. C. Redfern and K. Raghavachari, Gaussian-4 theory, *J. Chem. Phys.*, 2007, **126**, 084108.
34 L. A. Curtiss, P. C. Redfern and K. Raghavachari, Gaussian-4 theory using reduced order perturbation theory, *J. Chem. Phys.*, 2007, **127**, 124105.
35 M. J. Frisch, *et al.*, *Gaussian 16, Revision C.01*, Gaussian, Inc., 2016.
36 J. J. Fifen, Z. Dhaouadi and M. Nsangou, Revision of the Thermodynamics of the Proton in Gas Phase, *J. Phys. Chem. A*, 2014, **118**, 11090–11097.
37 R. Khare, S. S. Arora and A. Bhan, Implications of Cofeeding Acetaldehyde on Ethene Selectivity in Methanol-to-Hydrocarbons Conversion on MFI and Its Mechanistic Interpretation, *ACS Catal.*, 2016, **6**, 2314–2331.
38 J. S. Martínez-Espín, *et al.*, Hydrogen Transfer versus Methylation: On the Genesis of Aromatics Formation in the Methanol-To-Hydrocarbons Reaction over H-ZSM-5, *ACS Catal.*, 2017, **7**, 5773–5780.
39 S. Müller, *et al.*, Hydrogen Transfer Pathways during Zeolite Catalyzed Methanol Conversion to Hydrocarbons, *J. Am. Chem. Soc.*, 2016, **138**, 15994–16003.
40 A. Hwang and A. Bhan, Deactivation of Zeolites and Zeotypes in Methanol-to-Hydrocarbons Catalysis: Mechanisms and Circumvention, *Acc. Chem. Res.*, 2019, **52**, 2647–2656.
41 A. Hwang and A. Bhan, Bifunctional Strategy Coupling Y_2O_3-Catalyzed Alkanal Decomposition with Methanol-to-Olefins Catalysis for Enhanced Lifetime, *ACS Catal.*, 2017, **7**, 4417–4422.
42 M. DeLuca, C. Janes and D. Hibbitts, Contrasting Arene, Alkene, Diene, and Formaldehyde Hydrogenation in H-ZSM-5, H-SSZ-13, and H-SAPO-34 Frameworks during MTO, *ACS Catal.*, 2020, **10**, 4593–4607.
43 Y. Ji, *et al.*, Oxygenate-based routes regulate syngas conversion over oxide–zeolite bifunctional catalysts, *Nat. Catal.*, 2022, **5**, 594–604.

44 J. Zhang, *et al.*, Isolated Metal Sites in Cu–Zn–Y/Beta for Direct and Selective Butene-Rich C_{3+} Olefin Formation from Ethanol, *ACS Catal.*, 2021, **11**, 9885–9897.
45 D02 Committee, *ASTM D7566-24 'Standard Specification for Aviation Turbine Fuel Containing Synthesized Hydrocarbons'*, 2024.
46 V. L. Dagle, *et al.*, Single-Step Conversion of Ethanol to n-Butene over Ag-ZrO_2/SiO_2 Catalysts, *ACS Catal.*, 2020, **10**, 10602–10613.
47 M. A. Lilga, *et al.*, Systems and processes for conversion of ethylene feedstocks to hydrocarbon fuels, *US Pat.*, US20160194257A1, 2016.
48 S. Ding, H. Wang, J. Han, X. Zhu and Q. Ge, Ketonization of Propionic Acid to 3-Pentanone over $Ce_xZr_{1-x}O_2$ Catalysts: The Importance of Acid-Base Balance, *Ind. Eng. Chem. Res.*, 2018, **57**, 17086–17096.
49 A. Corma, V. Gómez and A. Martínez, Zeolite beta as a catalyst for alkylation of isobutane with 2-butene. Influence of synthesis conditions and process variables, *Appl. Catal., A*, 1994, **119**, 83–96.
50 M. L. Sarazen and E. Iglesia, Experimental and theoretical assessment of the mechanism of hydrogen transfer in alkane-alkene coupling on solid acids, *J. Catal.*, 2017, **354**, 287–298.
51 G. Yadav, *et al.*, Techno-economic analysis and life cycle assessment for catalytic fast pyrolysis of mixed plastic waste, *Energy Environ. Sci.*, 2023, **16**, 3638–3653.
52 R. J. Quann, L. A. Green, S. A. Tabak and F. J. Krambeck, Chemistry of olefin oligomerization over ZSM-5 catalyst, *Ind. Eng. Chem. Res.*, 1988, **27**, 565–570.
53 *Selective Catalysis for Renewable Feedstocks and Chemicals*, ed. K. M. Nicholas, Springer International Publishing, 2014.
54 D02 Committee, *D4054-23: Standard Practice for Evaluation of New Aviation Turbine Fuels and Fuel Additives*, 2023, DOI: 10.1520/D4054-21A, https://www.astm.org/cgi-bin/resolver.cgi?D4054-21A.